Chemical Physics Letters 501 (2010) 1–5

Contents lists available at ScienceDirect

Chemical Physics Letters

journal homepage: www.elsevier.com/locate/cplett

FRONTIERS ARTICLE

Precision cavity enhanced velocity modulation spectroscopy

Andrew A. Mills [a], Brian M. Siller [a], Benjamin J. McCall [a,b,*]

[a] Department of Chemistry, University of Illinois at Urbana-Champaign, 600 S. Mathews Avenue, Urbana, IL 61801, USA
[b] Department of Astronomy, University of Illinois at Urbana-Champaign, 1002 W. Green Street, Urbana, IL 61801, USA

ARTICLE INFO

Article history:
Available online 21 October 2010

ABSTRACT

The new technique of cavity enhanced velocity modulation spectroscopy has been further developed, incorporating a tighter cavity to laser lock and an optical frequency comb for absolute frequency calibration. Several N_2^+ transitions have been observed with much higher precision than previously possible, and transitions that were blended in earlier Doppler-limited experiments are now resolved. The full-width at half-maximum of the observed Lamb dips is $\sim$ 40 MHz, and appears to be dominated by a broadening due to the velocity modulation. Future extension of this technique into the mid-infrared should enable significant improvements in the sensitivity and resolution of vibrational spectroscopy of molecular ions.

1. Introduction

Ever since its development by Gudeman et al. in 1983 [1], velocity modulation spectroscopy has been the workhorse of molecular ion spectroscopy, because of its sensitive discrimination between ion and neutral signals [2]. In the past 25 years, this technique has been used to study nearly 50 different molecular ions, as reviewed in [3]. It has been implemented at wavelengths ranging from the UV to the millimeter-wave [4,5]. The most sensitive velocity modulation spectrometers (e.g., [6,7]) combine optical heterodyne modulation with a modified White cell for unidirectional multipassing. The S/N ratio of such experiments could be further improved by extending the optical path length using an external cavity, but the traditional 1*f* demodulated signal vanishes in such a cavity.

No major technological advances have been published on velocity modulation since it was last reviewed in [3]. However, additional molecular ions have been studied, including $FeCO^+$ [8] and FeO^+ [9] in the millimeter/submillimeter range, and D_2O^+ [10], SO^+ [11], and H_3O^+ [12] in the mid-infrared. Other molecules such as Cl_2^+ [13], CO^+ [14], and N_2^+ [15] have been studied in the visible/near-IR using the optical heterodyne magnetic rotation enhanced velocity modulation previously reviewed in [3].

In a recent Letter [16], we demonstrated that ion-neutral discrimination can be achieved in an optical cavity, using phase-sensitive 2*f* detection. This work also showed that Lamb dips were observable due to the high intracavity power, thus opening the door to routine sub-Doppler spectroscopy of molecular ions. However, those experiments were limited by a poor laser to cavity lock and a lack of precise frequency calibration. Here, we present an improved system that uses a double-passed acousto-optic modulator (AOM) to achieve a tight lock of the cavity to the laser, and an optical frequency comb to obtain precise frequency calibration.

We demonstrate the method using the well-studied N_2^+ ion, which is abundant in atmospheric aurorae and nitrogen discharges [17]. The $A^2\Pi_u - X^2\Sigma_g^+$ system has been studied extensively. Several bands were observed in auroral storms by Meinel in 1950 [18], and the 1–0 band was recorded in the laboratory by Benesh et al. in 1979 with a resolution of 1800 MHz [19]. Ferguson et al. recorded the Doppler-limited spectrum of several bands including the 1–0 band with a measurement precision of 60 MHz and an accuracy of 150 MHz [17]. These studies all relied on unmodulated sources, either DC positive column discharges or hollow cathodes. Other workers investigated higher vibrational levels by using velocity modulation [20–22].

Several groups [23–28] have used optical frequency combs to measure the absolute transition frequencies of molecular neutrals, in many cases combining them with sub-Doppler techniques to achieve a precision as good as $\sim$10 kHz. However, to our knowledge, the present Letter represents the first application of optical frequency combs to high-precision molecular ion spectroscopy.

2. Experimental setup

The experimental setup is an improved version of the one described in [16], and is illustrated in Figure 1. Molecular ions (N_2^+) were produced in an uncooled positive column discharge cell with a continuous flow of nitrogen at $\sim$0.5–4 Torr, as measured by a thermocouple gauge that was calibrated to a capacitance manometer. The ions were probed by the output of a Ti:Sapphire

* Corresponding author at: Department of Chemistry, University of Illinois at Urbana-Champaign, 600 S. Mathews Avenue, Urbana, IL 61801, USA.
E-mail addresses: aamills2@illinois.edu (A.A. Mills), bsiller2@illinois.edu (B.M. Siller), bjmccall@illinois.edu (B.J. McCall).
URL: http://bjm.scs.illinois.edu (B.J. McCall).

0009-2614/$ - see front matter © 2010 Elsevier B.V. All rights reserved.
doi:10.1016/j.cplett.2010.10.002

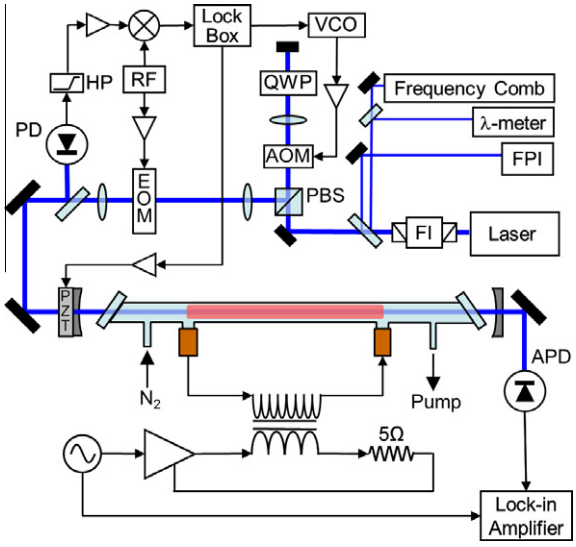

Figure 1. Experimental layout. Faraday isolator (FI), Fabry–Perot interferometer (FPI), acousto-optic modulator (AOM), polarizing beamsplitter (PBS), quarter-wave plate (QWP), radiofrequency generator (RF), electro-optic modulator (EOM), photodiode (PD), voltage controlled oscillator (VCO), avalanche photodiode (APD), high-pass filter (HP).

laser which was injected into an external cavity containing the discharge cell. An electro-optic modulator (EOM) added sidebands at 14 MHz, and the back-reflection off the cavity was used to generate a Pound–Drever–Hall error signal that represents the difference between the laser frequency and the cavity modes [29].

The low-frequency portion ($\lesssim 100$ Hz) of this error signal was fed back to a piezo on the cavity, which essentially locks the cavity to the laser; the laser itself is stabilized to an internal reference cavity which is temperature and pressure stabilized. The high-frequency portion of the error signal was fed to a voltage-controlled oscillator (VCO), which feeds a double-passed acousto-optic modulator (AOM; central frequency of 85 MHz) in a scheme similar to [30]. The frequency-shifted laser light was thereby locked to any fast fluctuations of the external cavity. This introduced a jitter of 1–2 MHz (as measured by fluctuations in the voltage input of the VCO while the system is locked), which is considerably smaller than the width of all of our observed transitions. The improved lock, compared to that in Ref. [16], enabled us to remove the intracavity iris which had been used to lower the finesse to ~ 100, resulting in a higher finesse of ~ 250 in the present experiment.

Before passing through the AOM (which blue-shifts the laser by 170 MHz), a portion of the laser beam was picked off and sent into a wavemeter (Bristol 621A-IR) with an accuracy of ± 0.2 ppm ($\sim \pm 65$ MHz), which was used for rough calibration. Another portion was combined on a photodetector with an optical frequency comb (MenloSystems FC1500), and the beat note was counted with the comb electronics. The FC1500 is a fiber-based comb, which contains two locking systems to keep the repetition frequency (f_{rep}) and the carrier-envelope offset (f_{ceo}) stabilized. In our case, f_{rep} was locked near 100.005 MHz, and f_{ceo} was locked to ~ 20 MHz. These frequencies are based on an input from a high-stability oven-controlled crystal oscillator that is disciplined to the Global Positioning System (Endrun Technologies Tycho, HS-OCXO). Since the oscillator control loop averaging time constant is over 500,000 s, the stability of the oscillator's 10 MHz frequency reference is expected to be better than 1×10^{-12}. The output of the fiber comb is frequency doubled in a periodically poled lithium niobate crystal, and spectrally broadened with a photonic crystal fiber. Because the comb light passes through a sum-harmonic generation periodically poled lithium niobate crystal, f_{ceo} becomes $2f_{ceo}$.

The output of the cavity was directed onto a photodiode, the signal from which was demodulated by a lock-in amplifier referenced to twice the plasma frequency (with the phase set to be optimally sensitive to ion signals). The output of the lock-in was recorded, along with calibration data, by a custom LabView program over the course of each scan.

Scanning was performed in two different modes, which we refer to as high resolution and ultra-high resolution. In the high resolution scans, the laser was stepped in 5 MHz steps, with a 300 ms time constant and a 300 ms delay between points, and calibration was performed using only the wavemeter. In the ultra-high resolution scans, the laser was stepped in 1 MHz steps, with a 1 s time constant and delay time, and was calibrated using the frequency comb. For this purpose, the data acquisition computer recorded f_{rep}, $|f_{ceo}|$, and $|f_{beat}|$ from the comb's computer, for each frequency step in our scans. Because the measurement system for $|f_{beat}|$ has a bandwidth of only 19.5–25.5 MHz, it was necessary to ratchet f_{rep} by 1.2 Hz whenever $|f_{beat}|$ approached its limit in the course of a scan. This ensured continuous measurements of the beat frequency against the same comb mode throughout an entire scan, which was typically 0.9 GHz in length. In the future, this 'soft lock' of the comb to the laser could be replaced by a system that directly locks the Ti:Sapphire laser to the comb; in such a scenario the laser could be scanned over long ranges simply by stepping f_{rep}.

The laser frequency can be determined using the equation $f_{Ti:S} = nf_{rep} + 2f_{ceo} + f_{beat}$. The difficulty in using the frequency comb for absolute calibration is that neither n (the comb mode participating in the beat) nor the signs of f_{ceo} and f_{beat} are known a priori. The sign of f_{beat} is easily determined by monitoring the change in $|f_{beat}|$ as the laser is tuned: if $|f_{beat}|$ increases as $f_{Ti:S}$ is increased, then its sign must be positive. The sign of f_{ceo} can only be determined by changing $|f_{ceo}|$ while watching $|f_{beat}|$ while the laser is held at a constant frequency. However, this last step was inadvertently omitted in the present experiment, so the sign of f_{ceo} is unknown in our measurements; however, all the ultra-high resolution scans reported here were recorded on two consecutive days, and the (unknown) sign of f_{ceo} was fixed by its lock, which was left on continuously during that period.

The value of the comb mode n was determined by using an estimate of $f_{Ti:S}$ from the wavemeter, which we call f_{wm}. For each possible sign of f_{ceo}, an estimate of n was calculated using $n_{\pm} = (f_{wm} \mp 2f_{ceo} - f_{beat})/f_{rep}$. These estimates can be expected to differ from an integer by an amount as large as 0.65, which represents the absolute accuracy of the wavemeter divided by f_{rep}. We found that in all cases only a single integer was within 0.65 of n_-, so that the determination of the true integer value of n_- was unambiguous. This was also true in some cases for n_+; these cases were used to determine the difference between f_{wm} and $f_{Ti:S}$ under the assumption that f_{ceo} is positive. We found that the wavemeter's offset varied by $\lesssim 8$ MHz over the course of a day, so that this could be used to 'calibrate' the wavemeter and unambiguously determine the integer value of n_+. For all scans, we found that $n_+ = n_- - 1$, and consequently the two possible values of $f_{Ti:S}$ for the two signs of f_{ceo} differ only by $f_{rep} - 2|2f_{ceo}| = 20.005$ MHz. For the remainder of this Letter, we adopt the value corresponding to a negative f_{ceo}, but we caution that all of our frequencies may be overestimated by 20.005 MHz as a result. In the future, this ambiguity can be resolved by a direct determination of the sign of f_{ceo} and/or by using a more accurate wavemeter. Nevertheless, the precision of the frequency determination at each step is ~ 1 MHz.

3. Transition frequencies

Ten transitions of the Q_{22} branch of the $v = 1 \leftarrow 0$ band of the Meinel system $A^2\Pi_u - X^2\Sigma_g^+$ of N_2^+ were observed in ultra-high

resolution scans. A representative set of high and ultra-high resolution scans of the $Q_{22}(14.5)$ line are shown in Figure 2. The vertical line represents the previously reported line center from the Doppler limited work of Ferguson et al. [17], and the horizontal line represents their stated calibration uncertainty (±150 MHz). Of the 10 observed transitions, eight were previously observed by [17], but $Q_{22}(0.5)$ and $Q_{22}(2.5)$ are reported here for the first time.

In the work of Ferguson et al. [17], many closely spaced transitions were unresolvable because of the Doppler-limited linewidths. Given the narrow sub-Doppler Lamb dips in the present Letter, many of these 'blended' transitions are now resolvable. For example, the $R_{11}(10.5)$ transition was previously blended with the stronger $Q_{22}(11.5)$ transition. As shown in Figure 3, the Lamb dips of these two transitions are clearly separated.

Each Lamb dip was fit to a Gaussian profile to determine the value of and the uncertainty in the line center frequency. Because of the relatively low S/N ratio of the wings of the Lamb dips, the profiles could be fit equally well to a Gaussian or a Lorentzian; a Gaussian fit was chosen because it was less sensitive to the noise in the wings of the observed dips. Table 1 shows our line center frequencies, the differences between these and the previous measurements, and the differences between our frequencies and the predictions of an effective Hamiltonian fit.

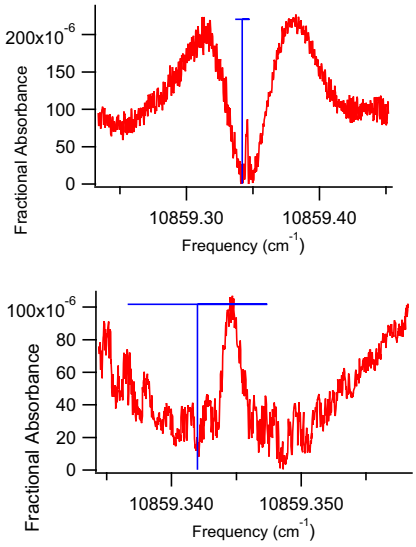

Figure 2. High-resolution (wavemeter calibrated) and ultra high-resolution (comb calibrated) scans of the $Q_{22}(14.5)$ line. The vertical line represents the previously reported line center [17]. The Lamb dip occurs within the uncertainties of the previous measurement, which is represented by the horizontal line.

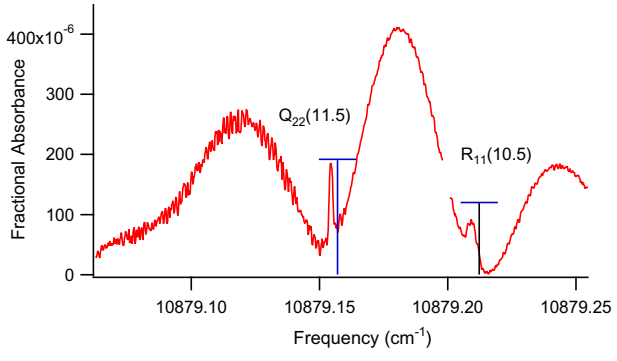

Figure 3. The high resolution scan of the $Q_{22}(11.5)$ line shows a second Lamb dip where the previously blended and unreported $R_{11}(10.5)$ line is now clearly resolved. The vertical line near $R_{11}(10.5)$ represents the predicted position from an effective Hamiltonian fit, and the horizontal bar indicates the rms-error of the Hamiltonian fit. The lock-in time constant was increased half-way through the scan which reduced the noise of the scan and broadened the observed $R_{11}(10.5)$ Lamb dip.

Table 1
Doppler free transition frequencies (in cm^{-1}) of the $Q_{22}(J)$ series calibrated with a frequency comb, as well as the differences from the previously published values [17], and the differences from an effective Hamiltonian fit using the spectroscopic constants from [17]. Note that the observed frequencies may be systematically too high by 20 MHz due to an ambiguity in the sign of f_{ceo} (see text).

J	Observed	Obs. – [17]	Obs.–Calc.
0.5	10924.65608(10)	–	0.00408
2.5	10919.46795(4)	–	0.00325
4.5	10912.92682(3)	0.00182	0.00322
6.5	10905.01953(3)	0.00853	0.00313
7.5	10900.54840(3)	0.00540	0.00310
8.5	10895.72876(3)	0.00076	0.00286
9.5	10890.55859(5)	0.00359	0.00299
11.5	10879.15394(3)	−0.00306	0.00294
12.5	10872.91398(3)	−0.00002	0.00288
14.5	10859.34469(3)	0.00269	0.00279

The differences between our line centers and those of [17] are reasonably small, but are in some cases larger than the previous work's estimated precision of about 0.002 cm^{-1} (which may apply only to the stronger transitions of [17]). The higher precision of the present Letter is evident from the residuals from the effective Hamiltonian fit (which used the constants from [17]). These residuals are tightly clustered around +0.003 cm^{-1}, with a standard deviation of 0.0004 cm^{-1}. This suggests that the molecular constants of this widely used prototype ion could be significantly improved using this method of sub-Doppler spectroscopy.

4. Linewidth investigation

In our initial report on cavity enhanced velocity modulation spectroscopy [16], the observed linewidth of the Lamb dips (~ 130 MHz) was dominated by the mechanical instability of the cavity, and the resulting frequency jitter in the laser (which was locked to the cavity). With our improved lock of the cavity to the laser, a considerably smaller Lamb dip linewidth (as low as 40 MHz) is observed. However, this width is still quite a bit larger than expected from pressure broadening, so we have investigated its dependence on the cell pressure, rotational level, and laser power.

A graph of the FWHM of the $Q_{22}(14)$ transition at several pressures between 0.5 and 4.5 Torr is shown in Figure 4. The calculated

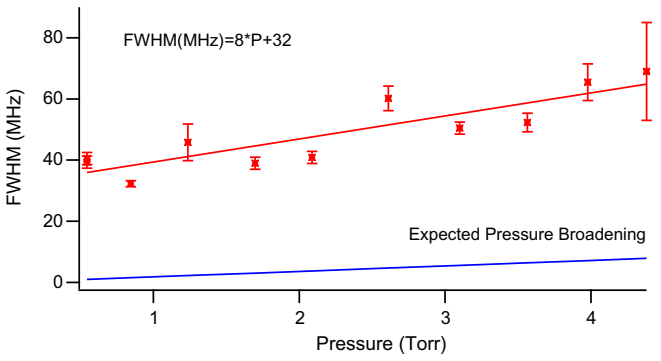

Figure 4. Linewidth as a function of cell pressure shows that the actual linewidth is much larger than the expected pressure broadening. Line of best fit: FWHM (MHz) = $8 \times p$(Torr) + 32.

pressure broadening coefficient, assuming a Langevin collision rate and using the formulas in [31], is approximately 1.8 MHz/Torr. Not only is the slope of the observed pressure dependence (8 MHz/Torr) much higher than this, but there is also a significant linewidth (32 MHz) even at the limit of zero pressure. Clearly an effect other than pressure broadening is dominating the observed linewidth.

To investigate the possible role of hyperfine structure on the observed linewidth, we measured transitions from many rotational states at the same pressure of 0.35 Torr. No change in the FWHM as a function of the rotational quantum number was observed. To check for power broadening, we measured the FWHM of the $Q_{22}(14.5)$ transition at incident optical powers between 7 and 30 mW, and observed no change over this range.

It seems clear that some other process is dominating the linewidth of the Lamb dips. We propose a lifetime broadening mechanism, based on the amount of time that a particular ion will be resonant with both counter-propagating laser beams (and thus participate in the Lamb dip) before its velocity is significantly changed by the AC field of the velocity modulation.

To estimate the order of magnitude of this effect, we assume that the drift velocity of the ions is proportional to the instantaneous voltage applied to the discharge cell. From the observed Doppler shift between the line center and the maxima of the velocity-modulated line profiles, we estimate the peak drift velocity to be $\sim 72\,000$ cm/s, which corresponds to a peak Doppler shift of ~ 800 MHz. In order for an ion to be probed by both directions of the laser beam in the cavity, its velocity along the cavity axis must be close enough to zero that its Doppler shift with respect to both beams is smaller than the cavity linewidth (~ 0.5 MHz). Since the Doppler shift changes from ~ 800 MHz to 0 MHz in one quarter of a discharge cycle (~ 6 μs), the ion has an effective 'lifetime' of only ~ 4 ns, which corresponds to a lifetime broadening of ~ 40 MHz, in rough agreement with our observations. The origin of the observed pressure dependence is unclear at the present time.

5. Saturation parameter

Figure 5 shows the experimentally observed Lamb dip depth as a function of the laser power incident on the cavity, which was adjusted by a variable attenuator on the RF input of the AOM (which changed its diffraction efficiency) while keeping all other experimental parameters constant. Theoretically [32], one would expect the ratio of the dip depth to the Doppler-limited absorption depth to be equal to $(1+S)^{-1/2}-(1+2S)^{-1/2}$, where S is the saturation parameter. Since the Doppler-limited absorption depth is independent of power, and S is proportional to the incident power, we fit the observed dip depth to the expression $A[(1+kP_{in})^{-1/2}-(1+2kP_{in})^{-1/2}]$. As seen in Figure 5, the fit is quite good; the resulting constant of proportionality is $k = 0.20 \pm 0.01\ \mathrm{mW}^{-1}$.

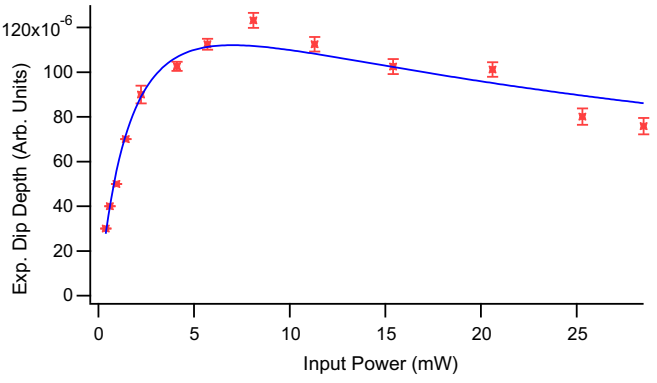

Figure 5. Experimentally observed Lamb dip depth, together with theoretical fit.

The saturation parameter S can be conveniently defined as Ω^2/Γ^2, where Ω is the angular Rabi frequency and Γ is the relaxation rate. Given that $\Omega = \mu E/\hbar$ (where μ is the transition dipole moment and E is the electric field strength), that the field intensity $I = E^2 c/8\pi$, and also that the field intensity inside the cavity can be expressed as $I = F\eta P_{in}/\pi r_0^2$ (where F is the cavity finesse, η is the coupling efficiency into the cavity [or the ratio P_{out}/P_{in}], and r_0 is the beam radius inside the cavity), we can write S in terms of P_{in} as

$$S = kP_{in} = \frac{8\pi}{ch^2}\frac{\mu^2}{\Gamma^2}\frac{\eta F}{\pi r_0^2}P_{in} \tag{1}$$

or, given an experimentally determined constant of proportionality k, we can write

$$\frac{\mu^2}{\Gamma^2} = k\frac{ch^2}{8\pi}\frac{\pi r_0^2}{\eta F}. \tag{2}$$

Substituting in the appropriate values for our case ($F = 250$, $\eta = 0.008$, $r_0 = 0.07$ cm, and $k = 2\times10^{-5}$ s erg^{-1}), we find that $\mu/\Gamma = 0.090$ Debye/MHz.

According to lifetime measurements [33], the Einstein coefficient for the 1–0 Meinel band is $\sim 7\times10^4\ \mathrm{s}^{-1}$; this is in good agreement with the theoretical value [34] of $5.9\times10^4\ \mathrm{s}^{-1}$. Combining this with the linestrength of the $Q_{22}(14)$ transition used for these measurements (computed from PGopher [35]), the transition dipole moment is expected to be $\mu = 0.38$ Debye. This suggests a relaxation rate $\Gamma \approx 4.2$ MHz. This demonstrates the ability of cavity enhanced velocity modulation Lamb dip spectroscopy to determine the ratio μ/Γ.

6. Conclusions and outlook

We have demonstrated that cavity enhanced velocity modulation spectroscopy can be used to make high precision (~ 1 MHz) measurements of molecular ion spectra, when used in conjunction with an optical frequency comb. This method provides considerably higher precision than conventional Doppler-limited spectroscopy, and consequently offers the prospect of more accurate determinations of molecular constants. Quantitative measurements of the Lamb dip depth also offer the possibility of experimentally determining ratios of transition dipole moments to relaxation rates.

Although our initial demonstration of this method has utilized an electronic transition of a molecular ion, we see no reason why this method could not be extended to vibrational spectroscopy in the mid-infrared. Typical vibrational dipole moments are on the order of 0.15 D, and this vibronic dipole moment was only 0.43 D, therefore the power density would only need to be about 10 times higher. This increased intracavity power could be achieved by using a higher finesse cavity or a higher power laser (e.g., a cw OPO). In such a case, frequency calibration could be performed either with a mid-infrared comb [36], or by upconverting the mid-infrared laser to the near-infrared by sum frequency generation with a stabilized Nd:YAG laser in a periodically poled lithium niobate crystal.

The widths of the Lamb dips are comparable to the kinematically compressed linewidths of ion beam instruments [37], therefore similar precision can be obtained with the current type of instrument. Ion beam instruments are considerably more complex and suffer from reduced ion density, but do offer other advantages, including simultaneous mass spectrometry, mass identification of spectral lines, and the possibility of rotational cooling when used with supersonic ion sources.

High-precision sub-Doppler vibrational spectroscopy of molecular ions would enable determination of molecular constants with near-microwave precision, which could in turn facilitate the prediction of pure rotational transitions. This could be very useful in reducing the classic 'search problem' in rotational spectroscopy, and could also facilitate astronomical observations of molecular ions that have not been measured in the microwave, sub-mm, or THz regions. Furthermore, the high precision of this method would facilitate the identification of four-line combination differences in complex spectra (such as, for example, CH_5^+ [38,39]) and thereby provide additional information to enable their assignment.

Acknowledgments

The authors are grateful to Prof. Benjamin Lev and Mr. Mingwu Lu for very helpful advice regarding laser locking electronics and techniques. This work has been supported by the NASA Laboratory Astrophysics program (NNX08AN82G), by an NSF CAREER award (CHE-0449592), by an Air Force Young Investigator award (FA9550-07-1-0128), and by the David and Lucile Packard Foundation.

References

[1] C.S. Gudeman, M.H. Begemann, J. Pfaff, R.J. Saykally, Phys. Rev. Lett. 50 (1983) 727.
[2] C.S. Gudeman, R.J. Saykally, Ann. Rev. Phys. Chem. 35 (1984) 387.
[3] S.K. Stephenson, R.J. Saykally, Chem. Rev. 105 (2005) 3220.
[4] W.Y. Fan, P.A. Hamilton, Chem. Phys. Lett. 230 (1994) 555.
[5] C. Savage, L.M. Ziurys, Rev. Sci. Instrum. 76 (2005) 043106.
[6] J.L. Gottfried, B.J. McCall, T. Oka, J. Chem. Phys. 118 (2003) 10890.
[7] C.P. Morong, J.L. Gottfried, T. Oka, J. Mol. Spectrosc. 255 (2009) 13.
[8] D.T. Halfen, L.M. Ziurys, Astrophys. J. 657 (2007) L61.
[9] D.T. Halfen, L.M. Ziurys, Chem. Phys. Lett. 496 (2010) 8.
[10] C. Duan, R. Zheng, S. Li, R. Wang, G. Huang, J. Mol. Spectrosc. 251 (2008) 22.
[11] S. Li, R. Zheng, G. Huang, C. Duan, J. Mol. Spectrosc. 252 (2008) 22.
[12] R. Zheng, R.-B. Wang, S. Li, G.-M. Huang, C.-X. Duan, Chin. Phys. Lett. 24 (2007) 2569.
[13] L. Wu, X. Yang, Y. Chen, J. Quant. Spectrosc. Radiat. Transfer 109 (2008) 1586.
[14] Y. Wu, X. Yang, Y. Guo, Y. Chen, J. Mol. Spectrosc. 248 (2008) 81.
[15] Y.D. Wu, J.W. Ben, L. Li, L.J. Zhen, Y.Q. Chen, X.H. Yang, Chin. J. Chem. Phys. 20 (2007) 285.
[16] B.M. Siller, A.A. Mills, B.J. McCall, Opt. Lett. 35 (2010) 1266.
[17] D.W. Ferguson, K.N. Rao, P.A. Martin, G. Guelachvili, J. Mol. Spectrosc. 153 (1992) 599.
[18] A.B. Meinel, Astrophys. J. 112 (1950) 562.
[19] W. Benesch, D. Rivers, J. Moore, J. Opt. Soc. Amer. 70 (1980) 792.
[20] M.B. Radunksy, R.J. Saykally, J. Chem. Phys. 87 (1987) 898.
[21] D.T. Cramb, A.G. Adam, D.M. Steunenberg, A.J. Merer, M.C.L. Gerry, J. Mol. Spectrosc. 141 (1990) 281.
[22] B. Lindgren, P. Royen, M. Zackrisson, J. Mol. Spectrosc. 146 (1991) 343.
[23] D. Mazzotti, S. Borri, P. Cancio, G. Giusfredi, P. De Natale, Opt. Lett. 27 (2002) 1256.
[24] Z.D. Sun, Q. Liu, R.M. Lees, L.H. Xu, M.Y. Tretyakov, V.V. Dorovskikh, Appl. Phys. B-Lasers and Optics 78 (2004) 791.
[25] I. Sherstov, S. Liu, C. Lisdat, H. Schnatz, S. Jung, H. Knockel, E. Tiemann, Eur. Phys. J. D 41 (2007) 485.
[26] P. Malara, P. Maddaloni, G. Gagliardi, P. De Natale, Opt. Exp. 16 (2008) 8242.
[27] S. Borri et al., Opt. Exp. 16 (2008) 11637.
[28] K. Takahata, T. Kobayashi, H. Sasada, Y. Nakajima, H. Inaba, F.-L. Hong, Phys. Rev. A 80 (2009) 032518.
[29] R.W.P. Drever, J.L. Hall, F.V. Kowalski, J. Hough, G.M. Ford, A.J. Munley, H. Ward, Appl. Phys. B-Photophys. Laser Chem. 31 (1983) 97.
[30] E.A. Donley, T.P. Heavner, F. Levi, M.O. Tataw, S.R. Jefferts, Rev. Sci. Instrum. 76 (2005) 063112.
[31] J.C. Pearson, L.C. Oesterling, E. Herbst, F.C. De Lucia, Phys. Rev. Lett. 75 (1995) 2940.
[32] K. Anzai, X.M. Gao, H. Sasada, N. Yoshida, Jap. J. Appl. Phys. Part 1-Regular Papers Brief Communications & Review Papers 45 (2006) 2771.
[33] J.R. Peterson, J.T. Moseley, J. Chem. Phys. 58 (1973) 172.
[34] F.R. Gilmore, R.R. Laher, P.J. Espy, J. Phys. Chem. Ref. Data 21 (1992) 1005.
[35] C.M. Western, Pgopher, a program for simulating rotational structure. http://pgopher.chm.bris.ac.uk, 2009.
[36] F. Adler, K.C. Cossel, M.J. Thorpe, I. Hartl, M.E. Fermann, J. Ye, Opt. Lett. 34 (2009) 1330.
[37] J.V. Coe, J.C. Owrutsky, E.R. Keim, N.V. Agman, D.C. Hovde, R.J. Saykally, J. Chem. Phys. 90 (1989) 3893.
[38] E.T. White, J. Tang, T. Oka, Science 284 (1999) 135.
[39] C. Savage, F. Dong, N.D.J., in: International Symposium on Molecular Spectroscopy 61st Meeting, talk TA5, The Ohio State University, Columbus, OH, 2006.

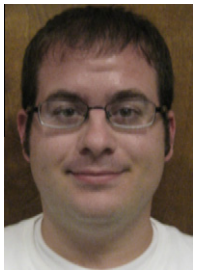

Andrew Mills graduated with a BS in Chemistry from Brigham Young University in 2005, and is currently a graduate student in Analytical Chemistry at the University of Illinois at Urbana-Champaign.

Brian Siller graduated with a BA in Chemistry, Computer Science, and Mathematics from Ohio Wesleyan University in 2007, and is currently a graduate student in Physical Chemistry at the University of Illinois at Urbana-Champaign.

Ben McCall received his PhD from the University of Chicago in Chemistry and Astronomy & Astrophysics. Following a Miller Research Fellowship at the University of California at Berkeley, he joined the faculty of the University of Illinois at Urbana-Champaign, where he is currently an Assistant Professor of Chemistry and Astronomy.